Early Triassic Neospathodus (Conodonta) apparatuses from the Taho Formation, southwest Japan

Author: Koike, Toshio

Source: Paleontological Research, 8(2) : 129-140

Published By: The Palaeontological Society of Japan

URL: https://doi.org/10.2517/prpsj.8.129

Paleontological Research, vol. 8, no. 2, pp. 129–140, June 30, 2004

Early Triassic *Neospathodus* (Conodonta) apparatuses from the Taho Formation, southwest Japan

TOSHIO KOIKE

36-6-606 Tokiwadai, Hodogaya-ku, Yokohama City, Japan, 240-0067

Received October 23, 2002; Revised manuscript accepted March 22, 2004

Abstract. Two conodont apparatuses, *Neospathodus symmetricus* Orchard, 1995 and *N. chionensis* (Bender, 1967) are reconstructed on the basis of the material from the Spathian (Lower Triassic) limestone in the Taho Formation of Ehime Prefecture, southwest Japan. The *Neospathodus* apparatuses are composed of eight types of elements: digyrate (cypridodelliform) M, alate S_0, digyrate (enantiognathiform) S_1, digyrate (grodelliform) S_2, bipennate $S_{3/4}$, angulate P_2, and segminate P_1 elements. This apparatus structure is the same as that for *Neogondolella* and is comparable to the standard 15-element plan of the Carboniferous ozarkodinids.

Key words: Gondolellidae, multielements, *Neospathodus*, Taho Formation, Triassic

Introduction

The genus *Neospathodus* Mosher includes a group of species possessing segminate P_1 elements with a well-developed anterior process; a posterior process that is short or absent (Sweet, 1973). *Neospathodus* was classified in the family Xaniognathidae Sweet (Sweet, 1981) and then assigned to the family Gondolellidae, together with the genus *Neogondolella* Bender and Stoppel (Sweet, 1988).

The species of *Neospathodus* are used as index fossils in the Lower Triassic (e.g., Orchard, 1995). There is, however, a controversy regarding components of the *Neospathodus* apparatus, namely, is it a unimembrate type or a multimembrate one?

Sweet (1970, 1988) regarded the apparatus of *Neospathodus* as a single-element (unimembrate) type composed of segminate (neospathodiform) Pa elements. On the other hand, Kozur (1976) believed that *Neospathodus* exhibits the same apparatus composition as *Gondolella* with six types of elements. He noted that ''Individual ramiform conodonts can, for the most part, be distinguished from those of *Gondolella* at the form species level; however, several forms cannot be separated at this level. The prioniodiniform (M) element differs only very slightly from apparatus to apparatus. Such a fact is not really remarkable because *Neospathodus* developed iteratively in several lineages by platform reduction from gondolellids.'' He did not, however, provide any more detailed information about the apparatus.

Orchard (1995) pointed out that at least one multielement apparatus of *Neospathodus* was tentatively reconstructed in his collections from Nevada, but whether that, or a different, apparatus could be recognized for other species was unknown.

I have undertaken a reconstruction of apparatuses of *Neospathodus* from the upper Spathian limestone in the Taho Formation exposed in Tahokamigumi, Sirokawa-cho, Higashiuwa-gun, Ehime Prefecture. The Triassic carbonate rocks of the formation are interpreted to have been deposited in an equatorial region of the Panthalassa Ocean (Ando *et al.*, 2001) and occur as a large exotic block in Jurassic clastic rocks (Koike, 1994). I present herein the systematic description of two multielement species of *Neospathodus*, *N. symmetricus* Orchard and *N. chionensis* (Bender) and offer a hypothetical arrangement of their skeletal architecture.

All of the described conodont specimens are housed in the Faculty of Education and Human Sciences, Yokohama National University, Yokohama.

Apparatus reconstruction of *Neospathodus symmetricus* Orchard

On the basis of rich conodonts from the Taho Formation, I reconstruct multielement apparatuses of *Neospathodus symmetricus* and *N. chionensis* which are composed of eight types of elements: digyrate (cypridodelliform) M, alate S_0, digyrate (enantiognathiform) S_1, digyrate (grodelliform) S_2, bipennate $S_{3/4}$,

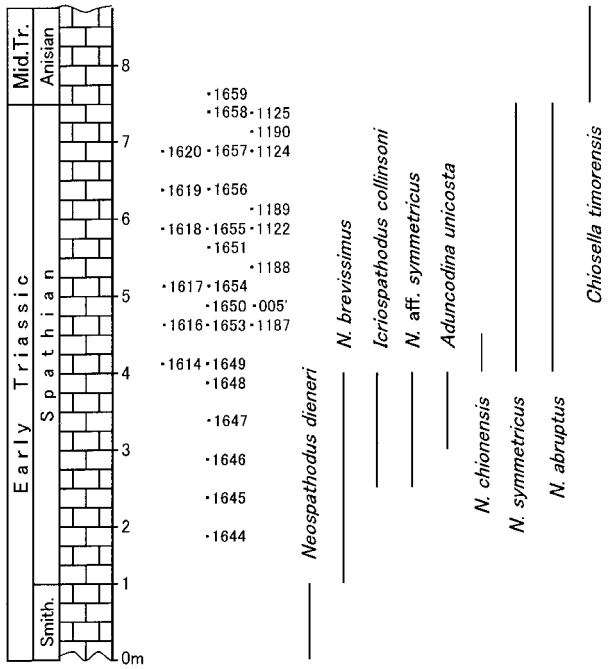

Figure 1. Stratigraphic section and vertical distribution of *Neospathodus symmetricus* Orchard 1995, *N. chionensis* (Bender, 1967) and important conodont species in the Taho Formation. Stratigraphic sections 005′, 1122–1125, 1187–1190, and 1644–1659 situated in the central part of the outcrop in Tahokamigumi. Stratigraphic section 1614–1620 situated at about 50 m east of section 1644–1659.

angulate P2, and segminate P1 elements. The apparatus nomenclature, S0 to S4, and P1 and P2, follows a proposal of Purnell *et al.* (2000).

The stratigraphic occurrence of *Neospathodus symmetricus* is restricted to the upper Spathian limestone in the Taho Formation (Figure 1). It ranges from the level at which *Icriospathodus collinsoni* (Solien) disappears through the Spathian-Anisian boundary at which *Chiosella timorensis* (Nogami) makes its debut.

The P1 element of *N. symmetricus* was proposed by Orchard (1995). Many specimens previously assigned to *N. homeri* P1 elements by several workers were regarded as *N. symmetricus* by Orchard (1995). Thus, previously described ramiform elements accompanied by *N. homeri* are possibly of the *N. symmetricus* apparatus.

Mosher (1968) recognized six species accompanied by *N. symmetricus* P1 elements [Mosher's *N. cristagalli* (Huckriede)] and "*Cypridodella unialata*" (S2 element of *N. symmetricus*). Among the six species, "*Cypridodella conflexa* Mosher", "*Diplododella magnidentata* (Tatge)", "*Enantiognathus ziegleri* (Diebel)", "*Prioniodina latidentata* Tatge", and "*Ozarkodina tortilis* Tatge" are similar to the M, S0, S1, S3/4, and P2 elements of the *N. symmetricus* apparatus of this study, respectively. "*Diplododella magnidentata*", "*P. latidentata*", and "*O. tortilis*" were, however, originally described based on the material from the Middle Triassic Muschelkalk by Tatge (1956). Kozur (1976) and Orchard and Rieber (1999) regarded the mentioned form species as elements of the Middle Triassic *Neogondolella mombergensis* (Tatge) apparatus. "*Enantiognathus ziegleri*" is probably the S1 element of the late Ladinian conodont apparatus, *Metapolygnathus* (*Budurovignathus*) *mungoensis* (Diebel) reconstructed by Mietto (1982). The holotype of "*Cypridodella conflexa* Mosher" was recovered from the upper Norian Hallstätter Kalk of Austria. All of the illustrated specimens of the six form species by Mosher (1968) are of Anisian age. Thus, the ramiform elements mentioned above are not part of the *N. symmetricus* apparatus.

Prior to Mosher (1968), Bender (1967) reported several Spathian conodont faunules accompanied by *N. homeri* and some ramiform elements from the island of Chios, Greece. Among three specimens illustrated as the species "*Apatognathus mitzopouli*" by Bender (1967), two of them agree morphologically with the S2 element of *N. symmetricus*. Bender's holotype of "*A. mitzopouli*" differs, however, from the S2 element. Other species accompanied by *N. homeri* are "*Ozarkodina tortilis*", "*Cypridodella muelleri* Tatge", and "*Enantiognathus ziegleri*". The illustrated specimens of these species are difficult to identify with the

Table 1. Occurrence of M, S_0, S_1, S_2, $S_{3/4}$, P_2, and P_1 elements of *Neospathodus symmetricus* Orchard obtained from 2 to 3 kg of limestone of the Taho Formation.

elements / level	M		S_0	S_1		S_2		$S_{3/4}$		P_2		P_1	
	S	D		S	D	S	D	S	D	S	D	S	D
005′	38	31	14	45	45	30	32	36	33	10	16	142	133
1125	36	34	18	34	33	29	30	22	21	18	21	167	153
1124	20	12	4	14	19	20	16	11	12	7	2	80	90
1122	25	15	15	32	25	22	19	24	24	20	11	98	99
1191	9	14	7	13	10	10	8	11	17	6	5	30	33
1190	11	7	2	9	10	10	5	10	9	5	4	39	42
1189	7	7	5	7	8	5	7	12	11	3	6	35	56
1188	29	28	8	17	23	20	32	24	26	19	6	86	85
1187	30	39	14	23	27	20	21	24	17	9	11	105	104
1658	10	7	9	10	9	12	11	6	9	9	8	27	26
1657	17	16	8	18	6	12	11	12	16	9	8	45	45
1656	27	27	10	26	18	25	26	32	29	19	21	75	82
1655	36	25	20	29	40	33	29	29	20	22	22	117	125
1654	12	16	14	9	12	9	15	14	12	11	11	37	31
1653	19	19	12	17	20	11	12	19	13	16	14	53	64
1651	16	16	7	14	16	20	13	16	13	15	8	75	89
1650	16	12	4	10	8	14	13	18	13	12	6	21	21
1619	21	20	20	23	17	19	18	20	23	18	16	78	78
1618	19	20	10	16	13	14	20	21	20	9	9	52	42
1617	48	42	19	35	34	39	36	37	38	15	24	150	152
1616	86	89	36	94	63	74	80	70	84	61	61	277	298
1614	12	8	11	19	18	13	7	18	16	14	17	49	50
total	544	504	267	514	474	461	461	486	476	327	307	1838	1898
total	1048		267	988		922		962		634		3736	
%	12.2		3.1	11.5		10.8		11.2		7.4		43.7	
ratio	2.3		0.6	2.1		2		2.1		1.4		8.1	

elements of *N. symmetricus* because of poor condition of the material.

Mosher (1973) proposed a multielement species *Ellisonia* sp. from the Spathian of Canada. *Ellisonia* sp. is composed of ''*Cypridodella unialata*'' (LC-element of Mosher, S_2 element of *N. symmetricus*), ''*C. conflexa*'' (LA), ''*D. magnidentata*'' (U), and ''*Hindeodella triassica* Müller'' (LB). Judging from Mosher's figures, ''*D. magnidentata*'' is similar to the S_0 element of *N. symmetricus*, but ''*C. conflexa*'' and ''*H. triassica*'' are dissimilar to the M and $S_{3/4}$ elements of the species.

The multielement species *Ellisonia clarki* of Sweet (1970) is similar to *N. symmetricus*. According to Sweet (1970), *E. clarki* occurs in the Spathian of the Salt Range and Trans-Indus Range in Pakistan, and is composed of four kinds of elements. The elements of *E. clarki*, U, LC, LA, and LB, correspond closely to the S_0, S_1, S_2, and $S_{3/4}$ elements of *N. symmetricus*. Sweet (1970), however, did not identify the LA element of *E. clarki* with ''*C. unialata* Mosher'' (S_2 element of *N. symmetricus*).

To sum up the above description, among eight element types of the *N. symmetricus* apparatus the P_1 and S_2 elements are identical to ''*N. symmetricus* Orchard'' and ''*C. unialata* Mosher'', respectively, but the other six types of elements are not identical to any previously proposed species with the exception of three elements (U, LC, and LB) of *E. clarki* Sweet.

The number of elements of *N. symmetricus* occurring in each level of the upper Spathian limestone of the Taho Formation is shown in Table 1. The frequency of M, S_0, S_1, S_2, $S_{3/4}$, P_2, and P_1 elements is 1048, 267, 988, 922, 962, 634, and 3736, respectively, and an approximate ratio of the elements is 2.3:0.6:2.1:2:2.1:1.4:8.1.

The ratio of the elements of M, S_0, S_1, S_2, S_3, S_4, P_2, and P_1 is 2:1:2:2:2:2:2:2 in a natural assemblage of *Neogondolella* sp. Rieber, 1980 (Orchard and Rieber, 1999) and in ozarkodinid apparatuses (*e.g.*, Aldridge *et al.*, 1987; Purnell and Donoghue, 1998; Purnell *et al.*, 2000). Compared with the ratio of the elements in *Neogondolella* sp. and ozarkodinid apparatuses, P_1 elements of *N. symmetricus* occur about four times as frequently as S_2 elements. The high abundance of P_1 elements is probably due to their robust constitution.

Table 2. Occurrence of P1 elements of *Neospathodus abruptus* Orchard, *N. brochus* Orchard, *N. curtatus* Orchard, *N.* sp. A, and *N.* spp. and ramiform elements probably of *N. abruptus*. These elements were obtained from 2 to 3 kg of limestone of the Taho Formation. Occurrence of *N. symmetricus and N. chionensis* is shown in Tables 1 and 3, respectively.

elements	*Neospathodus abruptus*?						*N. abruptus*	*N. brochus*	*N. curtatus*	*N.* sp. A	*N.* spp.
level	M	S_0	S_1	S_2	$S_{3/4}$	P_2	P_1	P_1	P_1	P_1	P_1
005′	2	1	2	1	5	2	28	1	1	13	4
1125	6	2	2	4	5	4	30	1	0	15	0
1124	2	0	3	0	3	3	23	1	0	6	0
1122	6	1	2	4	5	6	14	0	0	5	0
1191	3	1	3	3	2	2	3	0	0	1	0
1190	2	1	0	2	3	1	6	0	0	0	3
1189	2	0	0	0	0	3	5	2	0	3	0
1188	2	1	0	0	3	2	6	1	0	12	0
1187	3	2	0	1	2	2	12	0	0	1	0
1658	1	0	0	2	4	2	14	1	0	0	2
1657	1	1	2	4	7	3	17	0	0	2	1
1656	3	2	1	4	6	5	27	0	0	20	3
1655	5	1	3	4	4	5	42	0	0	10	0
1654	1	0	1	1	3	2	7	0	0	0	0
1653	3	1	1	2	4	5	6	0	0	4	0
1651	4	1	1	3	4	3	33	2	2	7	0
1650	1	0	2	1	2	1	3	0	1	5	1
1619	3	2	2	1	9	6	7	1	0	12	0
1618	2	1	0	2	0	2	5	0	0	3	0
1617	1	4	3	1	3	4	17	0	1	3	0
1616	8	3	3	10	17	8	65	1	0	10	0
1614	26	23	67	45	68	31	228	0	45	2	2
total	87	48	98	95	159	102	598	11	50	134	16

Similar occurrence of P1 elements is also recognized in the case of *Cratognathodus kochi* (Huckriede) (revised from *C. multihamatus* (Huckriede) of Koike, 1999) in the Taho Formation. The frequency of S_0 and $S_{3/4}$ elements is about half of what could be expected among ramiform elements. The low abundance of S_0 and $S_{3/4}$ elements is probably due to their fragility. I regard the *N. symmetricus* apparatus as composed of a single unpaired S_0, single pairs of M, S_1, S_2, S_3, S_4, P_2, and P_1 elements. The S_3 and S_4 elements are not distinguished from each other, because they show various transitional forms. Thus, I treat two single pairs of S_3 and S_4 elements as $S_{3/4}$ herein.

Neospathodus symmetricus occurs in the upper Spathian strata in the Taho Formation and is accompanied by two or three other species of *Neospathodus* in most levels. Table 2 shows the occurrence of the segminate P_1 elements and neospathid ramiform elements associated with *N. symmetricus* (Table 1), except for *N. chionensis* (Table 3) and *N.* sp. B mentioned on page 134.

The ramiform elements listed in Table 2 are probably of *Neospathodus abruptus* Orchard (Figure 2). The S_1, S_2, and $S_{3/4}$ elements are characterized by possession of thin and broad processes, and numerous denticles on the processes. The M elements possess a

Table 3. Occurrence of M, S_0, S_1, S_2, $S_{3/4}$, P_2 and P_1 elements of *Neospathodus chionensis* (Bender) obtained from 1 and 10 kg limestone of Levels 1649 and 1614, respectivery of the Taho Formation.

element	M		S_0	S_1		S_2		$S_{3/4}$		P_2		P_1	
level	S	D		S	D	S	D	S	D	S	D	S	D
1649	10	12	4	7	5	5	8	9	6	5	4	6	6
1614	52	57	63	54	50	55	56	87	72	50	50	60	60
total	62	69	67	62	55	60	64	96	78	55	54	66	66
ratio	0.92	1.03	1	0.92	0.82	0.9	0.96	1.43	1.16	0.82	0.81	0.99	0.99
total	131		67	117		124		174		109		132	
ratio	2		1	1.7		1.9		2.6		1.6		2	

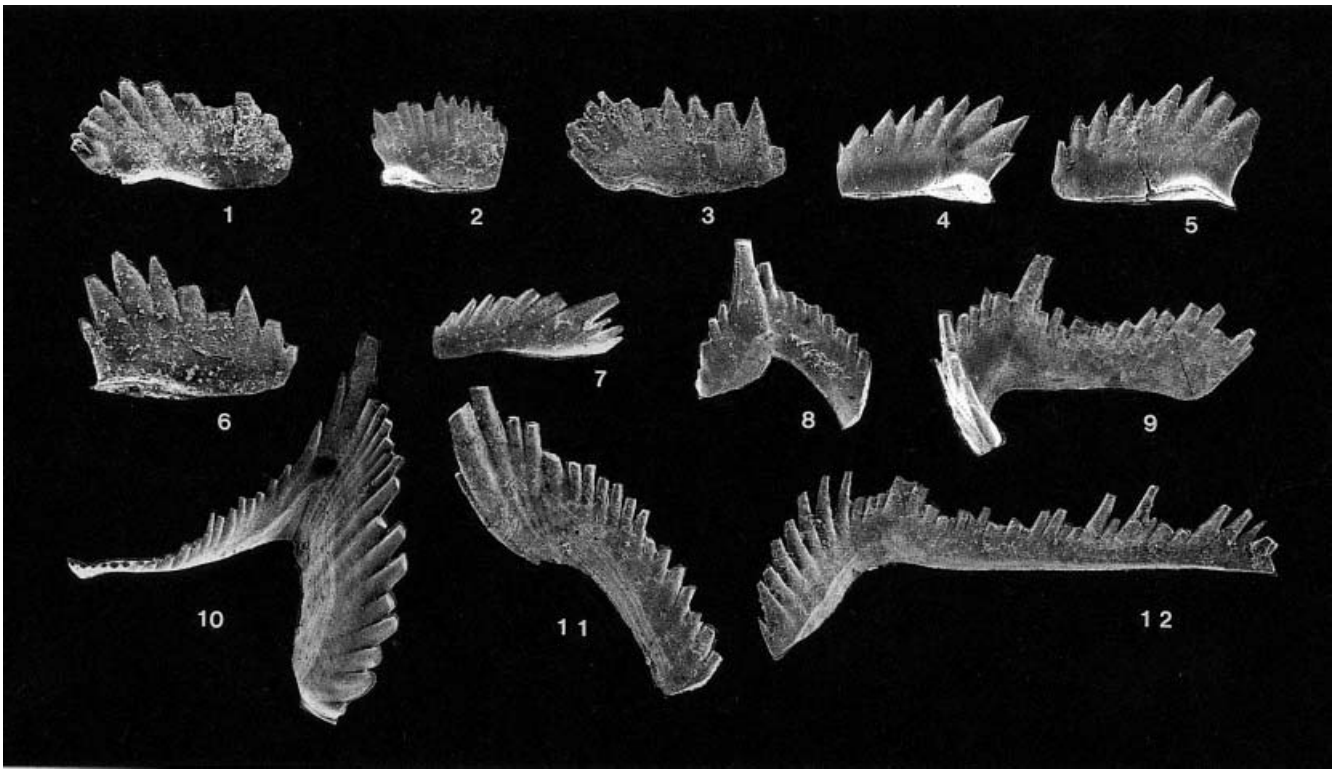

Figure 2. *Neospathodus* from the Taho Formation. **1**. *Neospathodus brochus* Orchard, 1995, P_1 element, YNUC16003 from Lev. 1616, inner view, ×50. **2**. *Neospathodus curtatus* Orchard, 1995, P_1 element, YNUC16004 from Lev. 1614, inner view, ×60. **3**. *Neospathodus* sp. **A**, P_1 element, YNUC16005 from Lev. 005′, inner view, ×50. **4**, **5**. *Neospathodus* sp. *N*. aff. *symmetricus* Orchard, 1995, P_1 elements, YNUC16006, 16007 from Lev. 1647, inner view, ×60. **6**. *Neospathodus abruptus* Orchard, 1995, P_1 element, YNUC16008 from Lev. 1614, inner view, ×50. **7–12**. *Neospathodus abruptus* Orchard?, 1995, from Lev. 1414, all ×50, 7: P_2 element, YNUC16009, inner view,. 8: M element, inner view, YNUC16010. 9: YNUC16011, S_0 element, lateral view. 10: S_1 element, inner view, YNUC16012. 11: S_2 element, YNUC16013, inner view. 12: $S_{3/4}$ element, YNUC16014, inner view.

relatively long outer lateral process with 5 to 6 denticles, and the P_2 elements have a relatively short posterior process with 2 to 4 denticles. I will describe *N. abruptus* in detail in the near future.

The P_1 element of *Neospathodus* sp. A is quite similar to that of *N. symmetricus* in outline of the unit and denticulation, but it possesses a very narrow slitlike basal cavity (Figure 2). These elements, however, probably fall within the range of intraspecific variation of *N. symmetricus* P_1 elements, because the degree of expansion of the basal cavity seems to be more variable than that described by Orchard (1995).

Unfortunately, it is impossible to discriminate the ramiform elements of *Neospathodus brochus* Orchard, *N. curtatus* Orchard, and *N*. spp. listed in Table 2, because of inadequate data in the present collection. Furthermore, another difficulty is in distinguishing the ramiform elements from those of *N. symmetricus*. The ramiform elements of *N. symmetricus* are inadequately preserved. Therefore, the frequency of ramiform elements of *N. symmetricus* listed in Table 1 may include a small number of elements of *Neospathodus brochus* Orchard, *N. curtatus* Orchard, and *N*. spp.

Apparatus reconstruction of *N. chionensis* (Bender)

The occurrence of *Neospathodus chionensis* is entirely restricted within about a 50 cm-thick ammonoid-bearing bed above the level where *Icriospathodus collinsoni* (Solien) disappears.

The M element is identical with ''*Ctenognathus chionensis*'' of Bender (1967). According to Bender, ''*C. chionensis*'' occurs in the upper Scythian of the island of Chios, Greece. ''*Ctenognathus chionensis*'' is accompanied by P_1 elements of *Neospathodus homeri* (Bender) and *N. triangularis* (Bender), and nine or ten types of ramiform elements. Bender (1967) illustrated one specimen of a *Neospathodus homeri* P_1 element (plate 5, figure 18) associated with ''*C. chionensis*''.

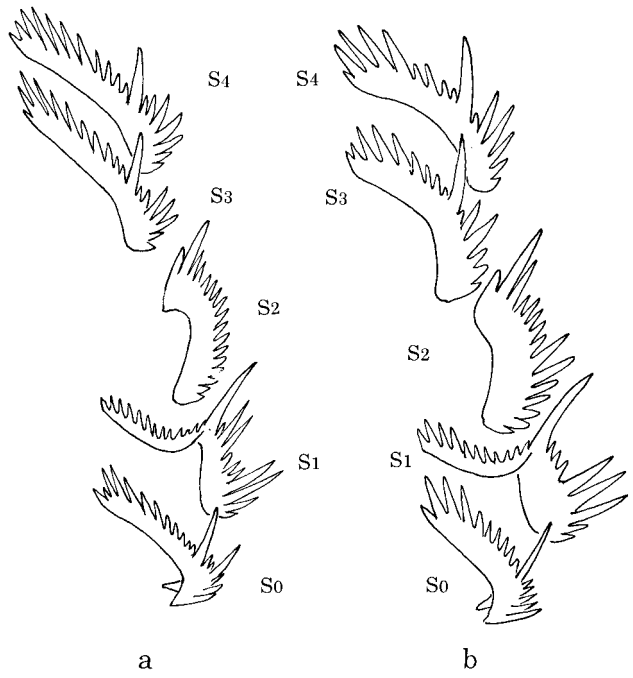

Figure 3. Hypothetical arrangement of S0 and sinistral S1, S2, and S3/4 elements of (a) *Neospathodus symmetricus* Orchard and (b) *N. chionensis* (Bender). The position and arrangement of the elements are based on the *Neogondolella* apparatus illustrated by Orchard and Rieber (1999) and the Carboniferous ozarkodinid *Idiognathodus* and *Gnathodus* apparatuses reconstructed by Aldridge *et al*. (1987), and Purnell and Donoghue (1997, 1998). The arrangement of S1 and S2 elements is based on my observation of *Neogondolella* sp. Rieber (1980).

The illustrated specimen cannot be assigned to *N. homeri* but it is certainly a Spathian *Neospathodus* and similar to P1 elements of a species of *Neospathodus* associated with *N. chionensis* in the Taho Formation. This species (*Neospathodus* sp. B) seems to possess eight types of elements that are characterized by large stout processes with isolated denticles. *Neospathodus* sp. B is restricted in occurrence in Level 1614 and easily distinguished from *N. chionensis*, *N. symmetricus*, *N. abruptus* and other *Neospathodus* species obtained from the level. Therefore, the frequency of elements of *N*. sp. B (25 specimens of P1 elements) is not listed in Table 2.

As far as I know, none of the seven types of elements including the neospathodiform P1 in the *N. chionensis* apparatus has been described. As mentioned above, the occurrence of this apparatus is restricted within a 50 cm-thick-bed. Thus, it is impossible to increase the reliability of the reconstruction on the basis of comparison of the occurrence of elements in various levels. I regard the reconstruction of *N. chionensis* as reasonable on the basis of the following facts: all the eight types of elements are characterized by possession of stout process with discrete denticles. Furthermore, their ratio of occurrence is not so different from that in a neogondolellid natural assemblage, as mentioned below.

The number of elements of *N. chionensis* obtained from two levels is listed in Table 3. The frequency of M, S0, S1, S2, S3/4, P2, and P1 elements is 131, 67, 117, 124, 174, 109, and 132, respectively, and an approximate ratio of the elements is 2:1:1.7:1.9:2.6:1.6:2. Consequently, I regard *N. chionensis* as a multielement apparatus composed of a single unpaired S0, single pairs of M, S1, S2, S3, S4, P2, and P1 elements. The S3 and S4 elements are also undistinguishable from each other as in the case of *N. symmetricus*.

The eight types of elements of *N. chionensis* and *N. symmetricus* apparatuses are very similar to each other in morphology. The presence of digyrate (enantiognathiform) S1 and digyrate (grodelliform) S2 elements in these apparatuses is common to *Neogondolella* (Orchard and Rieber, 1999) and *Cratognathodus kochi* (Huckriede) of Koike (1999). The apparatus structure of *Neospathodus* is comparable to the standard 15-element plan of ozarkodinids (Purnell and Donoghue, 1998; Purnell *et al*., 2000).

Systematic paleontology

Class Conodonta
Order Ozarkodinida
Superfamily Gondolellacea
Family Gondolellidae
Genus ***Neospathodus*** Mosher, 1968

Type species.—*Spathognathodus cristagalli* Huckriede, 1958.

Neospathodus chionensis (Bender, 1967)

Figure 5. 1–25

M element
Ctenognathus chionensis Bender, 1967, p. 503–504, pl. 1, figs. 13, 15, 16.

Diagnosis.—*Neospathodus chionensis* (Bender, 1967) is composed of single pairs of digyrate (cypridodelliform) M, digyrate (enantiognathiform) S1, digyrate (grodelliform) S2, bipennate S3/4, angulate P2, and segminate P1 elements, and a single unpaired alate S0 element. These elements are characterized by possession of stout processes and relatively discrete thick denticles.

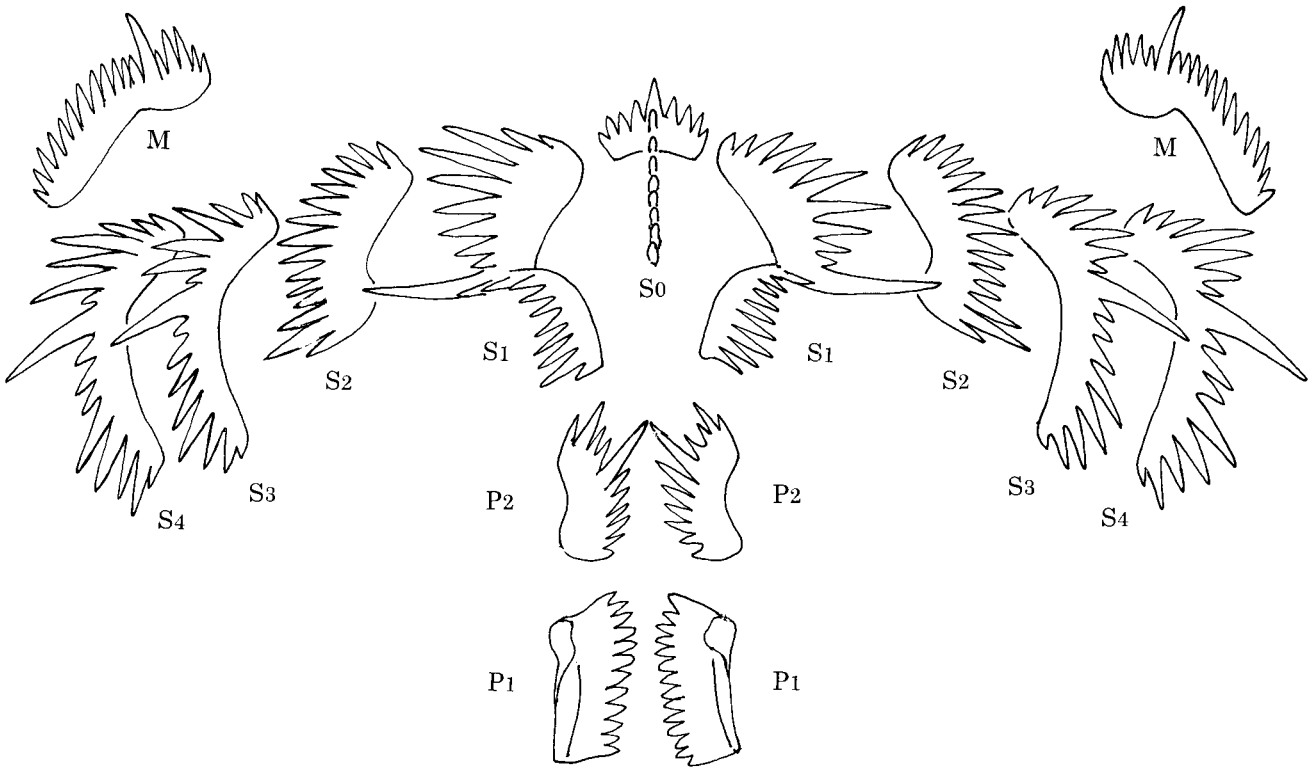

Figure 4. *Neospathodus chionensis* (Bender). Relative positions and schematic arrangement of component elements. This figure is based on the *Neogondolella* apparatus illustrated by Orchard and Rieber (1999). On the basis of my observation of *Neogondolella* sp. Rieber (1980), I arrange the S_1 and S_2 elements in each set with their inner-lateral process and the cusp directed in almost parallel to the posterior process and the cusp of the S_3 and S_4 elements.

Description.—P_1 element: Unit is stout, and ranges from 480 μm to 980 μm in length and from 240 μm to 530 μm in height. Ratio of length and height is 1.5–1.8:1. Denticles are 10 to 12 in number, subequal-sized, and upright in anterior and reclined in posterior portions. Upper surface of basal cup is thick on inner side. Basal cavity broadly expanded and quadrate to triangular in outline.

P_2 element: Anterior and posterior processes are almost equal in length and range from 240 μm to 370 μm and 250 μm to 380 μm in length, respectively. Both processes meet at an angle of about 140 to 160 degrees in upper view and 160 to 170 degrees in lateral view. Denticles on anterior process 5 to 7 in number, fused, and long, and tend to increase in height and inclination posteriorly. Denticles on posterior process 5 to 7 in number, discrete, short, and almost equal in size. Cusp is subequal to or much larger than largest denticles on anterior process. Basal cavity is slitlike and narrow groove extends toward anterior and posterior from basal cavity.

M element: Outer- and inner-lateral processes range from 210 μm to 470 μm and from 790 μm to 910 μm in length, respectively. Both processes meet at an angle of 120 to 150 degrees in lateral view. Outer-lateral process projects upward and flexed anteriorly and carries 1 to 5 relatively large discrete denticles. Inner-lateral process projects downward and curves posteriorly in distal portion. Denticles on inner-lateral process 12 to 15 in number, and tend to be long in middle portion and gradually increase in inclination proximally. Cusp is subequal to twice as long as largest denticle on processes. Basal cavity is small and triangular in shape with fine lip on inner side. Basal groove not observed.

S_0 element: Posterior process ranges from 510 μm to 780 μm in length. Each lateral process ranges from 270 μm to 430 μm in length. Lateral processes meet at cusp or first denticle anterior of cusp, and form an angle of 90 to 160 degrees to each other in antero-posterior view and 90 to 160 degrees on anterior side in upper view. Denticles on each lateral process 3 to 5 in number, discrete, and relatively large. Denticles on posterior process 7 to 10 in number, discrete, and increase in length and inclination posteriorly. Cusp large and may attain three times the length of the largest

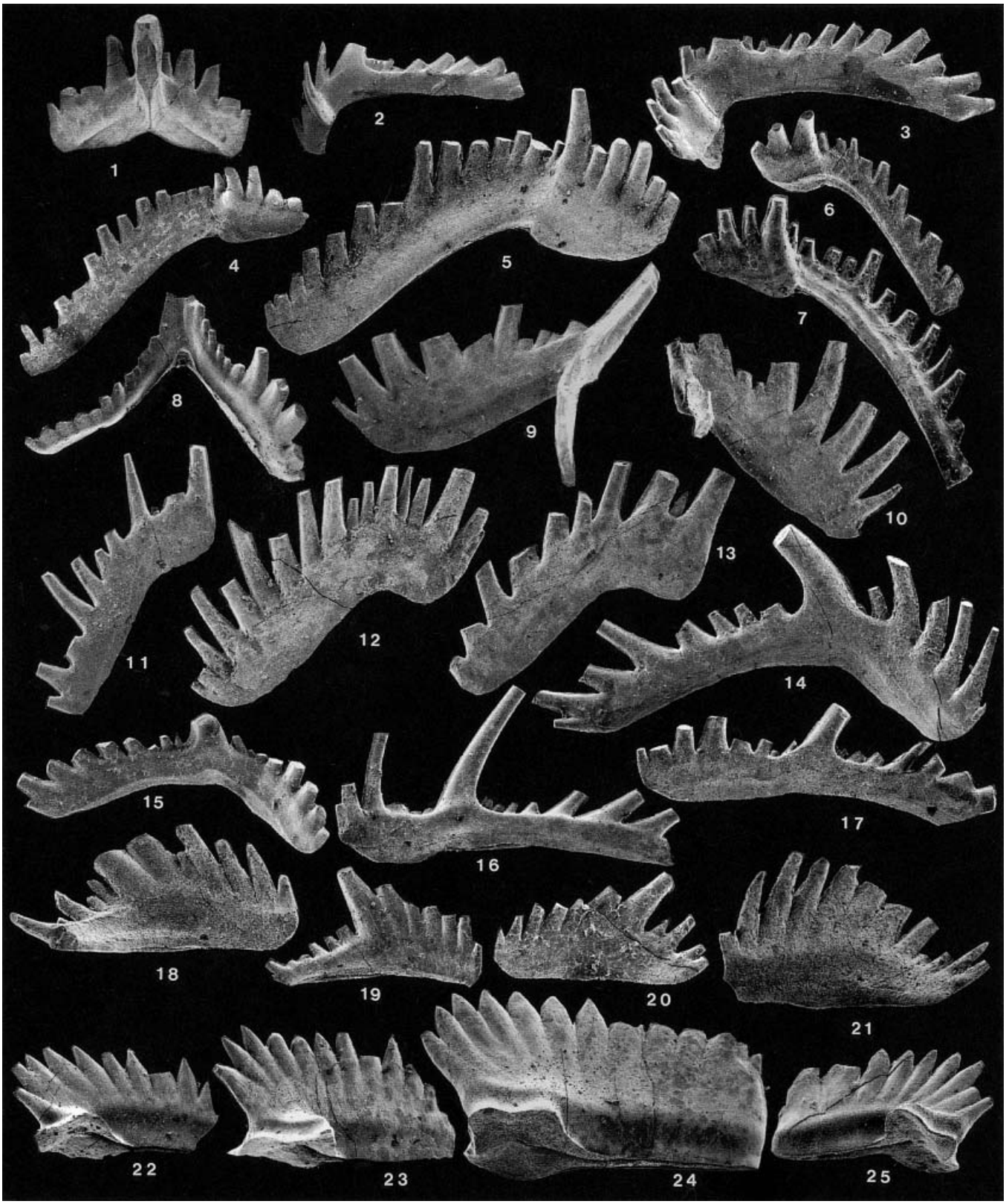

denticle on the lateral processes. Basal cavity indistinct and basal groove unobserved.

S1 element: Outer-lateral process ranges from 280 μm to 710 μm in length. Inner-lateral process ranges from 290 μm to more than 630 μm in length and is slightly longer than outer-lateral process. Both processes meet at cusp with an angle of about 60 degrees on upper view. Outer-lateral process ranges from 190 μm to 390 μm in height of blade, and somewhat convex inward. Inner-lateral process very low in height of blade, thin, and projects toward posterior and then curves and extends laterally. Denticles on outer-lateral process 7 to 11 in number, discrete, and incline toward cusp and inward forming a high convex crest in distal to medial portion. Denticles on inner-lateral process 12 to 15 in number and tend to increase in length and inclination distally. Cusp is as large as largest denticle on outer lateral process. Basal cavity indistinct and basal groove unobserved.

S2 element: Outer-lateral process ranges from 500 μm to 630 μm in length and from 210 μm to 270 μm in height of blade, and extends downward making an angle of 60 to 90 degrees with basal margin of cusp. Denticles 8 to 14 in number, discrete, and tend to be large in proximal to medial portion and increase in inclination proximally. One small denticle may be present on inner-lateral process. Zone of recessive basal margin commonly developed near basal part of cusp. Basal cavity indistinct and basal groove unobserved.

S3/4 elements: Anterior and posterior processes range from 380 μm to 430 μm and from 740 μm to 830 μm in length, respectively. Ratio of length of anterior and posterior processes is 1:1–2. Anterior process bends inward with an angle of 10 to 45 degrees and projects downward with an angle of 10 to 45 degrees. Number of denticles on both anterior and posterior processes is almost the same and ranges from 5 to 10. Denticles on anterior process tend to be large in size and decrease in inclination anteriorly. Cusp is subequal to twice as large as largest denticle on posterior process. Basal cavity indistinct and basal groove unobserved.

Remarks.—The P1 element of *N. chionensis* is characterized by possessing a stout blade and a cup with thick upper surface on inner side. *Neospathodus crassatus* Orchard is similar to the P1 element of *N. chionensis* but it is distinguished from the latter by having a few inwardly bending posterior denticles above the basal cavity.

Neospathodus symmetricus Orchard, 1955

Figure 6. 1–38

P1 element
Neospathodus symmetricus Orchard, 1995, p. 120, 121, figs. 2.6, 2.10–2.13, 2.18.
S0 element
Ellisonia clarki Sweet, 1970, p. 225, 226, pl. 4, figs. 17, 18. [U element]
S1 element
Ellisonia clarki Sweet, 1970, p. 225, 226, pl. 4, fig. 15. [LC element]
S2 element
Apatognathus mitzopouli Bender, 1967, p. 501, pl. 1, figs. 11, 14 (only)
Cypridodella unialata Mosher, 1968, p. 922, pl. 113, figs. 21, 27.
Ellisonia clarki Sweet, 1970, p. 225, 226, pl. 4, fig. 16. [LA element]
S3/4 element
Ellisonia clarki Sweet, 1970, p. 225, 226, pl. 4, fig. 19. [LB element]

Diagnosis.—*Neospathodus symmetricus* Orchard, 1995 is composed of single pairs of digyrate (cypridodelliform) M, digyrate (enantiognathiform) S1, digyrate (grodelliform) S2, bipennate S3/4, angulate P2, and segminate P1 elements, and a single unpaired alate S0 element. These elements are characterized by having a thin blade with fused denticles.

Description.—P1 element: Unit ranges from 260 μm to 790 μm in length and from 140 μm to 470 μm in height, respectively. Ratio of length and height is 1.5–2:1. Posterior and anterior ends may slightly curve inward. Denticles 8 to 15 in number, almost equal in size, and upright in anterior portion and increasingly reclined toward posterior. Basal cavity is broadly to narrowly expanded and basal groove extends toward anterior end.

P2 element: Anterior and posterior processes range from 130 μm to 350 μm and from 150 μm to 500 μm in length, respectively. Anterior process is commonly higher than posterior one. Both processes meet at an

Figure 5. 1–25. *Neospathodus chionensis* (Bender, 1967) from the Taho Formation. all ×50.
All from Lev. 1614 except for 11 from Lev. 1649. **1–3**, S0 elements. 1: YNUC16003, posterior view. 2, 3: YNUC16004, 16005, lateral views. **4–7**, M elements, inner views. 4, 5: YNUC16006, 16007, sinistral. 6, 7: YNUC16008, 16009, dextral. **8–10**, S1 elements. 8: YNUC16010, sinistral, upper view. 9: YNUC16011, dextral, inner view. 10: YNUC16012, sinistral, inner view. **11–13**, S2 elements, YNUC16013–16015, dextral, inner views. **14–17**, S3/4 elements. 14, 15: YNUC16016, 16017, sinistral, inner views. 16, 17: YNUC16018, 16019, dextral, inner views. **18–21**, P2 elements, inner views. 18, 19: YNUC16020, 16021, sinistral. 20, 21: YNUC16022, 16023, dextral. **22–25**, P1 elements, inner views. 22–24: YNUC16024–16026, sinistral. 25: YNUC16027, dextral.

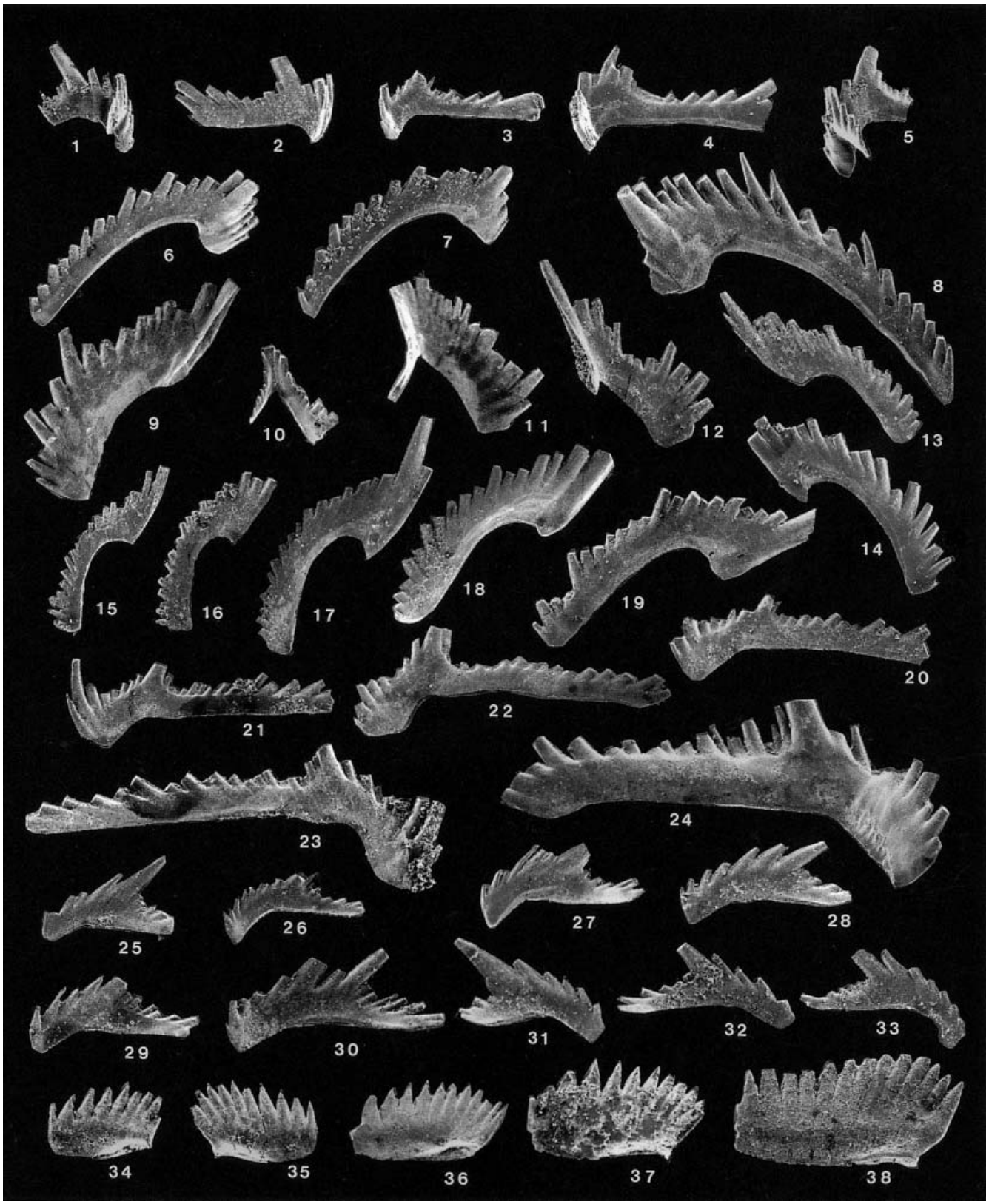

angle of 130 to 160 degrees in lateral view and 120 to 150 degrees in upper view. Denticles on anterior process 4 to 9 in number and increase in size and inclination posteriorly. Denticles on posterior process are 4 to 8 in number, and increase in size and inclination posteriorly. The ratio of number of denticles on anterior process to that on posterior one is 1:0.7–1.5. Cusp is larger than largest denticle on anterior process. Basal cavity minute and basal groove unobserved.

M element: Outer- and inner-lateral processes range from 50 μm to 210 μm and from 280 μm to 890 μm in length, respectively. Both processes meet at an angle of 60 to 120 degrees in lateral view. Outer-lateral process slightly flexed anteriorly and carries 1 to 5 short denticles. Inner-lateral process projects downward and curves posteriorly, and carries 14 to 20 equal-sized fused denticles. Cusp is twice to three times as long as denticle on inner-lateral process. Basal cavity and basal groove unobserved.

S0 element: Posterior process ranges from 330 μm to 630 μm in length. Lateral processes meet at cusp or the first or second denticle anterior of cusp and form an angle of 90 to 120 degrees in antero-posterior view and 120 to 170 degrees on anterior side in upper view. Denticles on each lateral process 2 to 3 in number, small, and fused. Denticles on posterior process 16 to 20 in number, fused, and increase in length and inclination posteriorly. Cusp is equivalent to or slightly larger than largest denticle on posterior process. Basal cavity indistinct and basal groove unobserved.

S1 element: Outer- and inner-lateral processes range from 190 μm to 410 μm and from 150 μm to 540 μm in length, respectively, and meet at cusp with an angle of about 60 degrees in upper view, and project downward. Outer-lateral process is deep and ranges from 280 μm to 370 μm in height of blade, and slightly convex inward. Inner-lateral process is thin, about 85 μm in height of blade, and directed toward posterior and then flexed and extending laterally. Denticles on outer-lateral process 10 to 16 in number, fused, incline proximally and inward, and form a high convex crest in distal to medial portion. Denticles on inner-lateral process up to 20 in number, small, and tend to increase in inclination and size distally. Cusp is slightly larger than largest denticle on anterior process. Basal cavity indistinct and basal groove unobserved.

S2 element: Outer-lateral process ranges from 290 μm to 530 μm in length and from 140 μm to 220 μm in height of blade, and extends downward approximately in parallel with axis of cusp. Denticles on outer-lateral process 15 to 20 in number, fused, subequal in size, and tend to increase in inclination proximally. One to three small denticles may be present on inner-lateral process. Cusp is subequal to twice as long as largest denticle on outer-lateral process. Basal margin near cusp curves shallowly to deeply. Basal cavity indistinct and basal groove unobserved.

S3/4 elements: Anterior and posterior processes range from 150 μm to 370 μm and from 420 μm to 1010 μm in length, respectively. Anterior process bends inward with an angle of 10 to 45 degrees and projects downward with an angle of 10 to 45 degrees. Denticles on anterior process range from 6 to 10 in number and tend to increase in size and decrease in inclination anteriorly. Denticles on posterior process range from 15 to 25 in number and tend to increase in size and inclination posteriorly. Cusp is subequal to twice as large as largest denticle on anterior process. Basal cavity indistinct and basal groove unobserved.

Remarks.—According to Orchard (1995), *N. symmetricus* is distinguished from *N. homeri* by having a shorter unit, fewer and more strongly reclined denticles, a more symmetrical basal cavity, and lacking a denticulate posterior process. P1 elements of *N. symmetricus* of the Taho Formation are identical to *N. symmetricus* described by Orchard (1995) in morphological characteristics. The segminate P1 elements of *N. homeri* revised by Orchard (1995) are entirely absent in the Taho Formation.

Neospathodus sp. aff. *N. symmetricus* Orchard, the

Figure 6. 1–38. *Neospathodus symmetricus* Orchard, 1995 from the Taho Formation. all ×60.

1–5, S0 elements, lateral views. 1: YNUC15965 from Lev. 1616, proximal. 2, 3: YNUC15966, 15967 from Lev. 1617. 4: YNUC15968 from Lev. 1655. 5: YNUC15969 from Lev. 1616, proximal. **6–8**, M elements, inner views. 6: YNUC15970 from Lev. 1616, sinistral. 7: YNUC15971 from Lev. 1655, sinistral. 8: YNUC15972 from Lev. 1614, dextral. **9–12**, S1 elements, inner views, sinistral except for 9. 9: YNUC15973 from Lev. 1614. 10: YNUC15974 from Lev. 1617. 11: YNUC15975 from Lev. 1614. 12: YNUC15976 from Lev. 1656. **13–19**, S2 elements, inner views. 13, 14, sinistral, 15–19, dextral. 13: YNUC15977 from Lev. 1619. 14: YNUC15978 from Lev. 1655. 15, 16: YNUC15979, 15980 from Lev. 1617. 17, 18: YNUC15981, 15982 from Lev. 1616. 19: YNUC15983 from Lev. 1617. **20–24**, S3/4 elements, inner views. 20–22, dextral. 23, 24, sinistral. 20: YNUC15984 from Lev. 1617. 21: YNUC15985 from Lev. 1656. 22: YNUC15986 from Lev. 1618. 23: YNUC15987 from Lev. 1616. 24: YNUC15988 from Lev. 1655. **25–33**, P2 elements, inner views. 25–30, dextral. 31–33, sinistral. 25: YNUC15989 from Lev. 1656. 26: YNUC15990 from Lev. 1617. 27: YNUC15991 from Lev. 1617. 28: YNUC15992 from Lev. 1619. 29: YNUC15993 from Lev. 1653. 30: YNUC15994 from Lev. 1616. 31: YNUC15995 from Lev. 1617. 32: YNUC15996 from Lev. 1655. 33: YNUC15997 from Lev. 1656. **34–38**, P1 elements, inner views. 34, 36–38, sinistral. 35, dextral. 34, 35: YNUC15998, 15999 from Lev. 1617. 36: YNUC16000 from Lev. 1614. 37: YNUC16001 from Lev. 1651. 38: YNUC16002 from Lev. 1614.

biostratigraphic occurrence of which is lower than that of *N. symmetricus* (Figure 1), resembles *N. symmetricus*, but it is distinguished from the latter in possessing a shorter P1 element with fewer denticles, and circular outline of the basal cup (Figure 2). The apparatus of this species probably consists of eight kinds of elements, the M element of which is distinguishable from that of *N. symmetricus* while the others are closely similar to those of the species.

On the basis of the morphological similarity of the P1 elements between *Neospathodus* and *Neogondolella*, Kozur (1976) and Sweet (1981) suggested that the two genera are phylogenetically related to each other. The common presence of enantiognathiform S1 and grodelliform S2 elements in the *Neospathodus* apparatuses and the natural assemblage of *Neogondolella* sp. Rieber, 1980 (Orchard and Rieber, 1999) provides an additional evidence for the view of Kozur (1976) and Sweet (1981).

Acknowledgments

I would like to express my sincere appreciation to Hisayoshi Igo, Emeritus Professor of Institute of Geoscience, University of Tsukuba, for his critical reading of the manuscript and valuable suggestions. I would like to acknowledge Peter von Bitter of Department of Palaeontology, Royal Ontario Museum, Canada and Mark A. Purnell of Department of Geology, University of Leicester, U.K. for their constructive comments on this manuscript.

References cited

Ando, A., Kodama, K. and Kojima, S., 2001: Low-latitude and Southern Hemisphere origin of Anisian (Triassic) bedded chert in the Inuyama area, Mino terrane, central Japan. *Journal of Geophysical Research*, vol. 102, p. 1973–1986.

Aldridge, R. J., Smith, M. P., Norby, R. D., and Briggs, D. E. G., 1987: The architecture and function of Carboniferous polygnathacean conodont apparatuses. *In*, Aldridge, R.J. *ed*., *Palaeontology of Conodonts*, p. 63–75. *British Micropalaeontological Society Series*, Chichester.

Bender, H., 1967: Zur Gliederung der Mediterranen Trias II. Die Conodontenchronologie der Mediterranen Trias. *Annales Géologiques des Pays Helléniques, Athènes, Laboratoire de Géologie de l'Université*, vol. 19, p. 465–540.

Huckriede, R., 1955: Die Conodonten in der Mediterranen Trias und ihr stratigraphischer Wert. *Paläontologische Zeitschrift*, vol. 32, no. 3/4, p. 141–175.

Koike, T. 1994: Skeletal apparatus and its evolutionary trends in a Triassic conodont *Ellisonia dinodoides* (Tatge) from the Taho Limestone, Southwest Japan. *Transactions and Proceedings of the Palaeontological Society of Japan, New Series*, no. 173, p. 366–383.

Koike, T., 1999: Apparatus of Triassic conodont species *Cratognathodus multihamatus* (Huckriede). *Paleontological Research*, vol. 3, p. 234–248.

Kozur, H., 1976: Paleoecology of the Triassic conodonts and its bearing on multielement taxonomy. *In*, Barnes, C.R., *ed*., *Conodont Paleoecology. Geological Association of Canada, Special Paper*, no. 15, p. 313–324. Waterloo, Ontario.

Mietto, P., 1982: A Ladinian conodont-cluster of *Metapolygnathus mungoensis* (Diebel) from Trento area (NE Italy). *Neues Jahrbuch für Geologie und Paläontologie, Monatshefte, 1982*, p. 600–606.

Mosher, L. C., 1968: Triassic conodonts from western North America and Europe and their correlation. *Journal of Paleontology*, vol. 42, p. 895–946.

Mosher, L. C., 1973: Triassic conodonts from British Columbia and the northern Arctic Islands. *Contribution to Canadian paleontology. Geological Survey of Canada, Bulletin*, vol. 222, p. 141–193.

Orchard, M. J., 1995: Taxonomy and correlation of Lower Triassic (Spathian) segminate conodonts from Oman and revision of some species of *Neospathodus. Journal of Paleontology*, vol. 69, p. 110–122.

Orchard, M. J. and Rieber, H., 1999: Multielement *Neogondolella* (Conodonta, upper Permian-middle Triassic). *Bollettino della Società Paleontologica Italiana*, vol. 37, p. 475–488.

Purnell, M. A. and Donoghue, P. C., 1997: Skeletal architecture and functional morphology of ozarkodinid conodonts. *Philosophical Transactions of the Royal Society, London, Series B*, vol. 352, p. 1545–1564.

Purnell, M. A. and Donoghue, P. C., 1998: Skeletal architecture, homologies and taphonomy of ozarkodinid conodonts. *Palaeontology*, vol. 41, p. 57–102.

Purnell, M. A., Donoghue, P. C. and Aldridge, R. J., 2000: Orientation and anatomical notation in conodonts. *Journal of Paleontology*, vol. 74, p. 113–122.

Rieber, V. H., 1980: Ein Conodontencluster aus der Grenzbitumenzone (Mittlere Trias) des Monte San Giorgio (Kt. Tessin/Schweiz). *Annalen des Naturhistorischen Museums in Wien*, vol. 83, p. 265–274.

Sweet, W. C., 1970: Uppermost Permian and Lower Triassic conodonts of the Salt Range and Trans-Indus Range, West Pakistan. *In*, Kummel, B. and Teichert, C. *eds*., *Stratigraphic Boundary Problems, Permian and Triassic of West Pakistan*, no. 4, p. 207–275. *The University of Kansas, Department of Geology, Special Publications*, Kansas.

Sweet, W. C., 1973: Genus *Neospathodus* Mosher, 1968, *In*, Ziegler, W. *ed*., *Catalogue of Conodonts*, vol. 1, p. 155–194. E. Schweizerbart'sche Verlagsbuchhandlung, Stuttgart.

Sweet, W. C., 1981: Family Xaniognathidae Sweet, 1981. *In*, Robinson, R. A. *ed*., *Treatise on Invertebrate Paleontology. Pt. W. Miscellanea, Supplement 2, Conodonta*, p. *W*154–*W*157. The Geological Society of America, Inc. and the University of Kansas Press, Boulder, Colorado and Lawrence, Kansas.

Sweet, W. C., 1988: The Conodonta: Morphology, Taxonomy, Paleontology, and Evolutionary History of a Long-Extinct Animal Phylum. *Oxford Monographs on Geology and Geophysics*, no. 10, 212 p. Clarendon Press, Oxford.

Tatge, U., 1956: Conodonten aus dem germanischen Muschelkalk. *Paläontologische Zeitschrift*, vol. 30, no. 1/2, p. 108–127, no. 3/4, p. 129–147.